Hydrogen Embrittlement of Magnesium and Magnesium Alloys: A Review

Journal of The Electrochemical Society, **160** (4) C168-C178 (2013)
0013-4651/2013/160(4)/C168/11/$31.00 © The Electrochemical Society

Hydrogen Embrittlement of Magnesium and Magnesium Alloys: A Review

Mariano Kappes,[a,b,*] Mariano Iannuzzi,[a,z] and Ricardo M. Carranza[b]

[a]*National Center for Education and Research on Corrosion and Materials Performance (NCERCAMP), The University of Akron, Akron, Ohio 44325, USA*
[b]*Comisión Nacional de Energía Atómica, Instituto Sabato (UNSAM/CNEA), Buenos Aires 1650, Argentina*

Magnesium and magnesium alloys are susceptible to stress corrosion cracking in various environments, including distilled water. There is compelling evidence to conclude that SCC is assisted, at least in part, by hydrogen embrittlement. This paper reviews the thermodynamics of the Mg-H system and the kinetics of hydrogen transport. Aspects of magnesium corrosion relevant to hydrogen absorption are also discussed. Crack growth mechanisms based on delayed hydride cracking, hydrogen adsorption dislocation emission, hydrogen enhanced decohesion, and hydrogen enhanced localized plasticity have been proposed and evidence for each of them is reviewed herein.
 [DOI: 10.1149/2.023304jes]

Manuscript submitted October 22, 2012; revised manuscript received January 16, 2013. Published February 26, 2013.

Pure magnesium is inherently susceptible to stress corrosion cracking (SCC)[1–3] and many of its alloys suffer SCC in environments considered innocuous for most other engineering alloys, e.g. distilled water.[4,5] In order to prevent SCC, some authors suggest that the applied stress has to be kept below 50% of the yield strength (YS),[6,7] reducing the attractiveness of Mg alloys for structural applications.

Pure magnesium[1–3,8] and magnesium-aluminum alloys[5,9–21] have received special attention in the literature. The susceptibility of magnesium alloys to SCC increases with increasing aluminum content,[17] a trend that is opposite to the beneficial effect of Al in stress-free corrosion rates.

Precipitation of β phase $Mg_{17}Al_{12}$ occurs in alloys with more than 2.1 wt% Al.[16] Since $Mg_{17}Al_{12}$ is nobler than the Mg-Al matrix,[11,22] precipitation of $Mg_{17}Al_{12}$ phase along grain boundaries[11,16,20] is thought to promote intergranular SCC (IGSCC) caused by preferential galvanic dissolution of the surrounding matrix.[16] The effect of second phase particles is discussed in detail in a separate section.

Extremely fast crack growth rates (i.e. in the order of 10^{-5} m/s) have been often reported for pure Mg[2] and Mg-Al alloys.[14,23] If cracking was entirely controlled by faradaic anodic dissolution, such crack growth rates would require anodic current densities in the order of 50 A/cm^2.[14] Therefore, most SCC models include some contribution of mechanical assisted fracture.

Even though there is compelling evidence supporting a hydrogen-assisted crack propagation mechanism,[1,2,13] there is no agreement regarding the exact nature of the H-metal-atom interactions leading to embrittlement. Mechanisms based on hydride formation, hydrogen enhanced decohesion, localized hydrogen enhanced plasticity, and hydrogen adsorption induced dislocation emission have been proposed and are reviewed in this paper. Validation of those mechanisms requires reliable hydrogen diffusion and hydrogen solubility data, which is also discussed herein.

The next sections present a critical review of the current state of knowledge on SCC of magnesium and magnesium alloys, with emphasis on hydrogen embrittlement mechanisms.

Thermodynamics of the Hydrogen–Magnesium System

Magnesium, a hydride-forming metal.— Mg and H form MgH_2,[24–26] a stoichiometric compound[27] that has a tetragonal structure[28] and decomposes at temperatures above 287°C[25] under a H_2 pressure of 101.3 kPa. In addition to its implications in SCC mechanisms, the formation of magnesium hydrides is of great interest to solid state hydrogen storage research.[24] The MgH_2 dissociation temperature, as well as other features of the Mg-H phase diagram, depend on the H_2 partial pressure.[26,27]

The nucleation and growth of MgH_2 during exposure of magnesium to gaseous H_2 at high pressure and temperature (~5 MPa and ~300–400°C) has been extensively studied[29–32] due to its application as a solid state hydrogen storage medium. Magnesium hydride has a high hydrogen absorption capacity, with a theoretical limit of 7.6 wt%. However, magnesium has a high temperature of hydrogen discharge[24] and slow absorption/desorption kinetics.[24,33,34]

Magnesium is combined with alloying elements by ball milling to enhance its hydriding/de-hydriding kinetics and to reduce the stability of the hydride.[24] Alloying with aluminum increases the kinetics of H absorption and desorption[33] during gas charging at 400°C and 3.8 MPa. Those properties were highest for a composition near that of $Mg_{17}Al_{12}$. This intermetallic compound, upon hydriding, decomposed into MgH_2 and Al, and the reaction was reversible upon dehydriding.[33]

Hydrogen solubility in Mg.— There are several complications in determining hydrogen solubility in magnesium. First, MgH_2, if formed as a surface layer, can limit the kinetics of hydrogen absorption[35,36] due to the extremely low diffusivity of hydrogen in MgH_2 (on the order of 10^{-16} m^2/s at 25°C [28]). Second, magnesium has a high vapor pressure and is volatile.[37,38] For example, as shown by Zeng and coworkers, a sample of magnesium can lose up to 1.5% of its weight during 1 h heating at 550°C.[37] Finally, a film of magnesium hydroxide, $Mg(OH)_2$ often present due to unintentional atmospheric exposure, can also hinder hydrogen absorption. $Mg(OH)_2$ decomposes to magnesium oxide (MgO) and hydrogen gas above 440°C.[28,39] Popovic[39] showed that a pre-heating at 600°C was necessary for hydrogen absorption at lower temperatures. This suggests that the hydroxide is more effective in blocking hydrogen ingress than the oxide.

San Martin and Manchester[26] and Okamoto[25] reviewed the Mg-H system in detail. The authors suggested that, at a H_2 pressure of 1 bar and in the temperature range between 175°C and the melting point (i.e. 650°C), H solubility was between 0.005 and 0.07 at%. The dependence of solubility with temperature (in at%) was given by:[26]

$$S(at\%) = 0.0023 + 1.28 \cdot \exp\left(\frac{22{,}780}{R \cdot T}\right) \quad [1]$$

Extrapolation to room temperature yields a solubility value of 0.002 at%. Table I summarizes reported hydrogen solubility values in magnesium.

Krozer and Kazemo[40] and Popovic et al.[39] reported that H solubility in Mg followed Sievert's law,[41] which states that hydrogen solubility in the metal lattice is proportional to the square root of the hydrogen partial pressure. In a recent review, Zeng et al.[37] stated that the reported heat of solution values for hydrogen in magnesium range between 20 and 24 kJ/0.5 mol H_2 for temperatures between 196 and

*Electrochemical Society Active Member.
zE-mail: mi@uakron.edu

Table I. Hydrogen solubility in pure Mg at atmospheric pressure.

Concentration			
at%	ppm	Observations	Reference
0.06	25	H Solubility at the melting point.	26
0.002	0.8	Extrapolated H solubility at room temperature (Equation 1).	26

645°C at a H_2 pressure of 101.3 kPa. This is a reasonable scatter based on the experimental difficulties.

A positive heat of solution value implies an endothermic reaction and, therefore, H solubility in Mg increases with temperature. However, thermodynamic modeling predicts that the heat of solution has a strong dependence with temperature in the 400 to 923 K (127 to 650°C) range, varying from 7 to 26 kJ/0.5 mol H_2.[37] The temperature dependence of the heat of solution invalidates the use of Equation 1 to estimate room temperature hydrogen solubility based on high temperature data.

Nishimura et al.[42] reported a value for the heat of solution of hydrogen in magnesium of 11.6 kJ/0.5 mol H_2 at 200–220°C, which is twice as high as the experimental values reported by other authors cited by Zeng et al.,[37] but it falls near the heat of solution predicted by the Zeng's thermodynamic model[37] in this temperature range. However, Nishimura et al.[42] deposited palladium (Pd) onto the oxidized Mg surface and conducted the experiments at a temperature high enough for interdiffusion of Mg and Pd[40] to take place, which might have affected heat of solution measurements. In this regard, Winzer et al.[23] found that the Nishimura et al.[42] results on hydrogen solubility exceeded those by Krozer and Kazemo[40] by 5 orders of magnitude.

Hydrogen Diffusion in Magnesium

Hydrogen transport by diffusion in the magnesium lattice is required for most cracking mechanisms based on hydrogen embrittlement. Literature results can be divided into high temperature and room temperature measurements; main findings for each temperature range are discussed below.

High temperature diffusivity measurements and extrapolations to room temperature.— In their pioneer work, Renner and Grabke[43] studied hydrogen diffusion kinetics in cerium-containing magnesium alloys by measuring the thickness of the layer containing cerium hydrides, in the 425–525°C temperature range. Extrapolation of those results to room temperature by Atrens et al.[44] yielded a value of 10^{-13} m^2/s.

Nishimura et al.[42] studied the permeation of gaseous hydrogen through Pd-coated pure magnesium disks at temperatures near 200°C. As previously discussed, at this temperature Mg and Pd interdiffusion is significant.[40] Another issue of Nishimura's sample preparation method is that the deposition of Pd occurred on top of the air-formed oxide layer. This oxide layer can interfere with H permeation measurements, a fact that is well known from hydrogen permeation studies conducted in steels.[45] The authors reported a diffusion coefficient value of H in Mg (D_H^{Mg}) of

$$D_H^{Mg}\left(m^2 \cdot s^{-1}\right) = 1.54 \cdot 10^{-6} \cdot \exp\left(\frac{24{,}100}{R \cdot T}\right) \quad [2]$$

where R is the universal gas constant and T the temperature in K. The value did not depend on the input pressure of hydrogen, suggesting independence on H concentration. Extrapolation of this equation to room temperature yields a D_H^{Mg} value of 1×10^{-10} m^2/s. As a reference, for carbon steels, where H permeation has been well characterized, values for the lattice hydrogen diffusion coefficient in steel, D_H^{Fe}, at room temperature are on the order of 10^{-10} m^2/s to 10^{-8} m^2/s,[46,47] depending on the microstructure and composition of the steel. Atrens[44] relied on the extrapolated value to room temperature as supporting evidence for transport of H ahead of a stress corrosion crack. Extrapolation to room temperature of the experimental results of Nishimura et al. and the ab initio computer simulations by Schimmel et al.[48] yielded a similar value,[44] which was more than 3 orders of magnitude higher than extrapolated results[44] obtained by Renner and Grabke at higher temperature.[43]

Room temperature measurements.— Spatz et al. reported a value of $D_H^{Mg} = 1.1 \times 10^{-20}$ m^2/s based on the growth kinetics of hydride layers formed on magnesium surfaces near room temperature (i.e. 32°C).[35] Growth of hydrides controlled by hydrogen diffusion in the magnesium lattice is implicit in the calculations conducted by the authors.

Knotek et al.[49] studied the diffusion of hydrogen in magnesium and other candidate alloys for hydrogen storage applications using the Devanathan and Stachurski[50] approach at room temperature. In this method, a fixed hydrogen concentration is maintained on one side of a metallic thin sheet using a split-cell. This side of the cell is either polarized to a fixed cathodic potential or left at the open circuit potential (OCP or E_{OC}). In contrast, the other side is anodically polarized at a potential several hundreds of mV above the reversible potential of the hydrogen reduction reaction (HRE), $E^{REV}(H^+/H_2)$, so that diffusing H is rapidly oxidized to H^+ [51] at the exit side of the metallic sheet. This oxidation current gives a direct indication of the hydrogen flux through the sheet of metal. Knotek et al.[49] used 6 M KOH on the cathodic side and N,N′-dimethylformamide on the anodic side of the cell. This organic compound, as stated by the authors, minimized Mg corrosion while maintaining a sufficient ionic conductivity. Under a charging current of 1 mA/cm^2, a value of 6.7×10^{-13} m^2/s was obtained for D_H^{Mg}. The value is in accord with extrapolations to room temperature[44] of the Renner and Grabke[43] results. However, hydrogen had to diffuse through the air formed hydroxide or oxide layer present on the anodic side of the membrane, and probably through a hydride layer on the cathodic side of the membrane. This could lead to a lower apparent D_H^{Mg} value.

Other authors[9,52] have estimated the hydrogen diffusion coefficient solely based on mechanical tests conducted at room temperature. Makar et al.[9] calculated D_H^{Mg} based on the time required to observe embrittlement in unstressed Mg-9 wt% Al samples exposed to chromate/chloride mixtures. Dietzel et al.[52] also estimated D_H^{Mg} after modeling failure of AZ91* Mg-Al-Zn alloy in distilled water. Both investigators coincided in a value for D_H^{Mg} of 2×10^{-13} m^2/s.

Table II summarizes the available information on D_H^{Mg} at room temperature. Figure 1 shows available information on D_H^{Mg} discussed in this section, compared with literature results from other hexagonal close packed (hcp) metals.[53] Table II and Figure 1 shows that there is high dispersion in the results, suggesting that more research is necessary to elucidate hydrogen diffusion kinetics at room temperature.

Aspects of Magnesium Corrosion Relevant to Hydrogen Embrittlement

Breakdown of surface films and hydrogen absorption.— A $Mg(OH)_2$ film spontaneously covers the surface of Mg and its alloys when exposed to alkaline environments,[54–57] which provides some corrosion protection. This film might also form in weakly buffered environments where surface pH can increase due to corrosion and

*if no UNS numbers were given, the commercial alloy name reported by the authors was used.

Table II. Summary of available information on the hydrogen diffusion coefficient in magnesium at room temperature.

D_H^{Mg} (m^2/s)	Method	Alloy	Reference
10^{-13}	Extrapolation to room temperature of Renner and Grabke[43] results.	Mg-Ce alloy	44
10^{-9}	Extrapolation to room temperature of Schimmel[48] results.	Pure Mg	44
10^{-9}	Extrapolation to room temperature of Nishimura[42] results.	Pure Mg	44
1.1×10^{-20}	Kinetics of hydride layer growth at 32°C.	Pure Mg	35
6.7×10^{-13}	Devanathan and Stachurski[50] approach	Pure Mg	49
2×10^{-13}	Estimations based on mechanical tests	AZ91 and Mg 9 wt% Al	9, 52

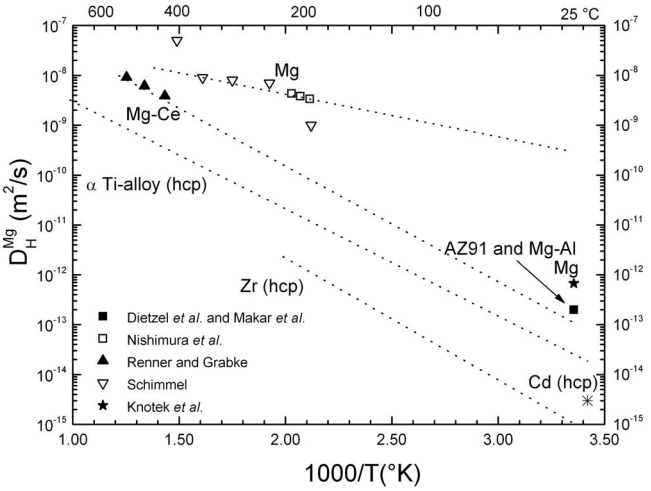

Figure 1. Reported values for the hydrogen diffusion coefficient in magnesium and magnesium alloys compared to other hexagonal metals, adapted from[53] with permission of Woodhead Publishing Limited.

hydrogen evolution.[7,58] As shown by Stampella,[1] atomic hydrogen cannot permeate through a Mg surface covered by $Mg(OH)_2$. Assuming a similar behavior to iron, where it is well known that protective films hinder hydrogen absorption,[59,60] this could be related to an extremely low hydrogen diffusion coefficient value through the hydroxide layer.[61]

In the presence of aggressive anions such as chloride or sulfate, film breakdown results in high corrosion rates.[55–57] For single phase alloys, film breakdown occurs in local spots that extend radially with time exhibiting hydrogen evolution.[57,62–64] Given that the open circuit potential of magnesium in chloride solutions, which is on the order of -1.4 V_{SHE},[22,65] is about 20 mV[58] higher than the breakdown potential,[56,57] localized dissolution of magnesium is sometimes referred to as pitting.[56,57] However, unlike autocatalytic pits in aluminum and stainless steels,[66] pits in Mg remain very shallow, with no clear tendency to grow in depth.[58] In any case, localized corrosion provides both an active oxide-free layer and sites for hydrogen reduction. Therefore, localized corrosion is a pre-requisite for hydrogen embrittlement.[1,3,67]

Mechanical rupture of surface films.— Plastic deformation of surface grains can also result in the breakdown of the surface film.[68] In this case, strain rate determines the rate of creation of bare metal.[20] The amount of hydrogen absorbed by the lattice is, therefore, controlled by a tradeoff between strain rate and re-filming reactions.[9,69]

Thermodynamic stability of hydrides in the presence of water.— Perrault[70] constructed a potential-pH phase diagram for the magnesium-water system that included magnesium hydrides, in addition to Mg, H_2O, Mg^{++} and $Mg(OH)_2$ species first considered by Pourbaix.[71] Figure 2 summarizes Perrault's phase diagram. As seen in

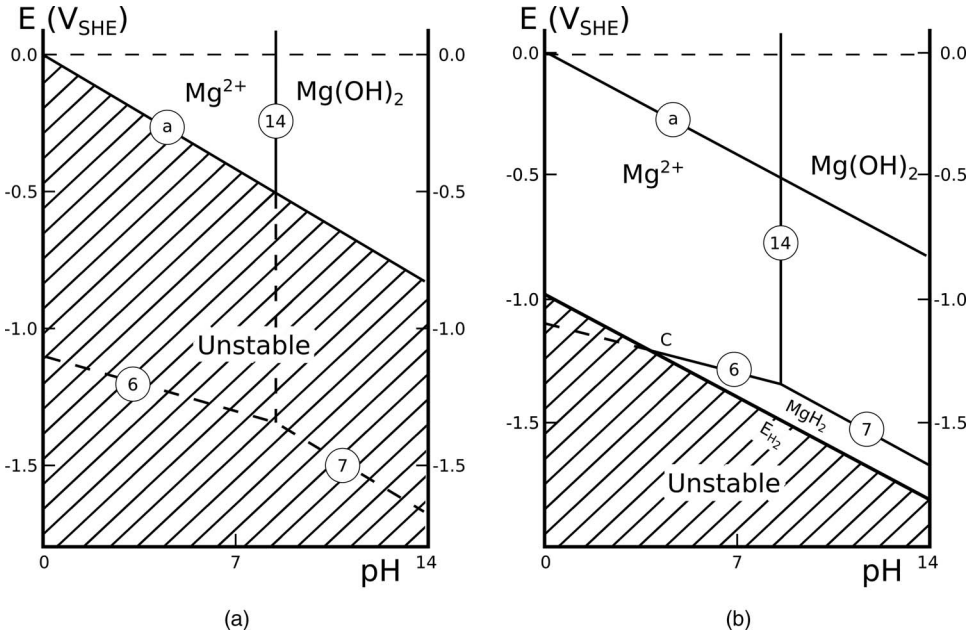

Figure 2. Potential-pH phase diagram for the magnesium-water system, showing stability domains of each species in aqueous solutions (a) and under a hydrogen overpotential of 1 V, and (b) considering $[Mg^{+2}] = 1M$ and hydrogen pressure = 1 atm.[70] Lines show equilibrium of the following reactions: a) $2H^+ + 2e^- = H_2$, 6) $Mg^{+2} + 2H^+ + 4e^- = MgH_2$, 7) $Mg(OH)_2 + 2H^+ + 4e^- = MgH_2 + 2OH^-$, 14) $Mg(OH)_2 = Mg^{+2} + 2OH^-$. (From reference 70, J. Electroanal. Chem. Interfacial Electrochem., Vol. 51, G. Perrault, "The potential-pH diagram of the Magnesium-water system" p. 107 (1974). Reproduced with permission of Elsevier Science).

Figure 2a, hydrides are thermodynamically unstable in the presence of Mg^{++}. An equilibrium potential is not observed on the magnesium electrode, unless the hydrogen overpotential on the surface of the electrode is greater than 0.843 V vs. SHE. Figure 2b shows the stability domains considering a hydrogen overpotential of 1 V. In this case, under a net cathodic overpotential, an equilibrium potential in presence of hydrides can be expected at a pH greater than 5 (point C).

Perrault[72] stated that a cathodic film might form in a magnesium electrode, probably composed of magnesium hydride and magnesium hydroxide. However, magnesium hydride is a strong reducer and unstable in the presence of water, decomposing to Mg^{+2} or $Mg(OH)_2$.[72] These results suggest that magnesium hydride might be present as an intermediate reaction product during corrosion.

Evidence of MgH_2 formation during magnesium corrosion.—Several authors claim to have detected the presence of MgH_2 in corroded pure magnesium[73–76] and in AZ91 Mg-Al-Zn alloys.[77] Gulbrandsen[73] identified the four strongest lines of MgH_2 on the X-ray diffraction (XRD) pattern of the deposit formed on a pure magnesium electrode exposed to HCO_3^-/CO_3^{2-} buffer polarized below -2.5 V_{SCE}. The strongest peak of the hydride phase was also seen in the corrosion product formed at E_{OC}, suggesting that the phase is present in smaller amounts under these conditions. Since MgH_2 is unstable in the presence of water,[70] the author[73] recognized that the hydride product is continuously consumed at the metal/electrolyte interface. Brun et al.[75] also identified MgH_2 in an XRD scan performed on magnesium alloy exposed to 3 wt% NaCl at a cathodic potential.

Seyeux et al.[74] exposed magnesium to pure water and detected fragments of MgH_2 by Time of Flight-Secondary Ion Mass Spectroscopy (ToF-SIMS). The signal was maximum at 10-nm inside the film, but the authors recognized that the phase was in small amounts compared to MgO and $Mg(OH)_2$ and not detectable by XPS.

Hydrogen absorption during corrosion.— Chakaprani and Pugh[13] exposed Mg-7.5 wt% Al samples to $NaCl/K_2CrO_4$ solutions at room temperature to investigate the degradation of mechanical properties after hydrogen charging. According to the authors, the corrosion potential measured in this solution was about -1.26 V_{SHE}.[11] At this potential, based on Sievert's law, a high hydrogen fugacity[6] is expected on the surface of the corroding electrode, resulting in high hydrogen solubility.[39,40] The authors also measured total absorbed hydrogen using the inert gas fusion method. In this method, the specimen is melted under a flow of inert gas in a graphite crucible. Dissolved hydrogen is then released and the flowing gas analyzed in a thermal conductivity or infrared cell.[78] The method is purely comparative. A reliable measurement requires the use of standards with known hydrogen content. As shown by the authors, the H concentration reached values on the order of 170 ppm or 0.41 at% after 24 h of exposure. Nevertheless, it is important to highlight that the hydrogen concentration obtained by this method possibly included hydrogen present in solid solution, hydrides, and traps.[78]

Morozova[79] exposed various magnesium alloys to water vapor for 30 days and determined that the amount of hydrogen increased from about 20 ppm to 100 ppm, or 0.049 to 0.24 at%. For his work, Morozova used the vacuum hot extraction method.[80] In this method, the H-charged sample is heated in vacuum and the evolving gas is forced through a liquid nitrogen trap to eliminate water vapor and then analyzed to determine H content.[80] It was previously stated that the maximum hydrogen solubility in solid pure magnesium, measured at the melting point, was approximately 25 ppm or 0.06 at%.[25,26] Chakaprani and Pugh[13] and Morozova[79] results show that it is possible to exceed this amount by environmental exposure.

Other authors[81–83] used hydrogen collection experiments to indirectly estimate the amount of hydrogen absorbed by magnesium. Hydrogen collection experiments involve measuring the volume of hydrogen evolved during corrosion with an inverted burette.[58] The authors[81–83] observed that, when using the weight loss of magnesium or the measured current, the volume of hydrogen evolved during open circuit corrosion,[81] under an applied cathodic potential,[82] or under a net anodic current,[83] was less than what would have been expected from Faraday's law. One problem with those investigations is that all authors assumed[81–83] that the difference between the expected and the measured volume of hydrogen was only related to the amount of hydrogen absorbed by the metal, neglecting the solubility of hydrogen in the solution at equilibrium with the atmospheric hydrogen pressure present in the inverted burette. For example, using the values quoted by Kirkland et al.,[84] the solubility of hydrogen gas in H_2O at 37°C is 1.4 mg kg^{-1} and the density of hydrogen gas at the same temperature is approximately 9×10^{-5} g mL^{-1}. Therefore, 15 mL of hydrogen per kilogram of solution would remain dissolved in the corroding solution at the end of the experiment. Since the solubility of hydrogen in the solution increases with a decrease in temperature, the hydrogen solubility at 25°C should be approximately 17.4 mL/kg of water.[85] The amount of hydrogen remaining in solution is expected to be on the same order of magnitude and, in some cases, higher than the volume of hydrogen collected at the end of the corrosion experiment.[81] Besides hydrogen dissolution in the corroding solution, there are other sources of error in estimating corrosion rates using hydrogen evolution measurements, including non-faradaic dissolution, as reviewed by Kirkland et al.[84] Kirkland et al. stated that collection efficiencies can be on the range of 60% of the amount corresponding to magnesium weight loss. This should be interpreted as a limitation of the technique and not as hydrogen absorption by the lattice.

States of hydrogen in magnesium.—The results by Chakrapani and Pugh[13] and Morozova[79] discussed above suggest that environmental exposure of magnesium samples could result in H concentrations that exceed its solubility limit. Reported hydrogen concentrations for steels are also several times larger than the lattice solubility in iron,[86] with excess hydrogen occupying trap sites such as grain boundaries, dislocation lines, and interfaces. It is probable that magnesium might exhibit a similar behavior. However, hydrides are thermodynamically stable in this system, which constitutes a significant difference.

Chakrapani and Pugh[13] used vacuum annealing to investigate the distribution of hydrogen in Mg-7.5 wt% Al samples. Vacuum annealing was performed at 385°C for 4h, which is well above the MgH_2 decomposition temperature.[13,25] As shown by the authors,[13] the amount of hydrogen decreased to 50 ppm after vacuum annealing a sample previously charged with 170 ppm of H in a $NaCl/K_2CrO_4$ solution. This result suggests that a significant fraction of hydrogen was: i) in solid solution, ii) in hydrides that decomposed at such high temperature or iii) in reversible traps.

There are various hypotheses to explain the residual hydrogen detected after a vacuum treatment including irreversibly trapped hydrogen, hydrogen gas blisters, and hydrogen present in corrosion products.[5] In a similar experiment, Chen[77] suggested that the remnant hydrogen measured after annealing above the hydride decomposition temperature was present as a gaseous phase.

The 50 ppm value can be compared to residual hydrogen contents reported by Chino et al.[87]. In their work, pure magnesium samples with different residual hydrogen contents were obtained by modifying the degassing time of the melt before casting the ingots, which resulted in samples with a hydrogen concentration between 16 and 35 ppm.[87] Secondary ion mass spectrometry (SIMS) revealed that, at these concentrations, hydrogen was mainly segregated at triple joint grain boundaries.[87] Impurity H concentration values around 10 ppm were reported by Mallet et al. in unexposed commercially pure magnesium.[80] Table III summarizes reported hydrogen concentration values in Mg and Mg alloys.

Hydrogen absorption at anodic and cathodic potentials.—Some researchers have suggested that hydrogen absorption is favored at anodic rather than cathodic potentials.[1,69,88] However, those authors based their conclusions solely on mechanical results in which the observed ductility loss was higher at anodic overpotentials. To the best of our knowledge, no detailed hydrogen concentration measurements have been reported for magnesium samples under anodic or cathodic overpotentials to date, despite the scientific relevance that those measurement could have in the materials and corrosion communities.

Cathodic overpotentials prevent localized corrosion, which is required for hydrogen absorption as discussed in *Breakdown of surface*

Table III. Hydrogen concentration in magnesium measured by different processes as indicated.

Concentration				
at%	ppm	Observations	Alloy	Reference
0.039–0.085	16–35	Obtained by changing degassing time of the melt. H mainly segregated at grain boundaries.	Pure Mg	87
~0.049–0.24	~20–100	Measured before and after exposure to water vapor for 30 days.	Mg-Al, Mg-Al-Mn	79
0.41	170	Measured after corrosion for 24 hr in $NaCl/K_2CrO_4$ solution.	Mg- 7.5 wt% Al	13
0.12	50	Corroded for 24 hr in $NaCl/K_2CrO_4$ solution, and then exposed to vacuum at 385°C for 4h.	Mg- 7.5 wt% Al	13

films and hydrogen absorption. Furthermore, based on studies by Perrault,[70,72] MgH_2 and $Mg(OH)_2$ films might develop at the surface during cathodic polarizations, preventing hydrogen absorption.

Anodic potentials, on the other hand, favor localized corrosion and disruption of the protective film that prevents hydrogen absorption. Tunold et al.[57] suggested that film-free magnesium areas increased with the polarizing current during anodic polarization. Hydrogen evolution from pit bottoms is frequently observed for other metals, including iron, titanium and aluminum, which is caused by the reduction of H^+ to H_2(g) inside pits.[89,90] Several authors[1,6,57,58,63,69,81,83,91] support that hydrogen evolution in magnesium increases with anodic overpotential, a phenomenon commonly referred to as "negative difference effect". However, this is a topic of much controversy and several mechanisms were proposed for explaining this behavior, as reviewed by others.[1,57,91] Furthermore, recent galvanostatic studies[92] conducted in pure magnesium exposed to chloride solutions suggested that hydrogen evolution did not increase with the applied anodic current, based purely on visual observations. It is not the authors' intention to review this topic in depth, other than stating that hydrogen is likely to be absorbed and embrittle the alloy if produced at the metal interface. One explanation for the negative difference effect is related to Mg dissolving into Mg^+ in film-free areas above the pitting potential.[58,63,91] It is postulated that Mg^+ later reacts with water to produce hydrogen gas (H_2) according to

$$2Mg^+ + 2H_2O = 2Mg^{2+} + H_2 + 2OH^- \quad [3]$$

However, it is not clear whether this reaction occurs homogeneously in the solution or at the electrode interface. If produced homogeneously, hydrogen gas could only embrittle the alloy if it is transported to the electrode by diffusion, followed by dissociation at the metallic interface. Mg^+ was not directly detected in solution,[63] and several authors questioned the validity of this mechanism,[62,92–94] supporting the notion that magnesium dissolves directly as Mg^{++}.[62,92–94]

Evidence Supporting Hydrogen Embrittlement Mechanisms

In this section, results from SCC tests that suggest contributions due to hydrogen embrittlement are discussed. Hydrogen can be present in the lattice as a result of environmental exposure prior to testing, leading to internal hydrogen embrittlement.[95] Alternatively, hydrogen can be absorbed by the lattice during testing, causing environmental hydrogen embrittlement.[95]

Internal hydrogen embrittlement.— Pre-exposure to gaseous hydrogen.—AZ91 magnesium samples pre-charged in a hydrogen atmosphere at 300°C and 3 MPa and subsequently tested in air failed just above YS,[21] Figure 3. A control sample received the same heat-treatment but under an argon atmosphere, and failed with considerable plastic deformation, similar to a sample tested in air with no heat-treatment. The sample heat treated in hydrogen exhibited a decrease in ductility of 80% and a decrease in ultimate tensile strength (UTS) of 50% with respect to the sample heat treated in argon, Figure 3. Application of the inert gas fusion method to the samples pre-charged in gaseous hydrogen[5,21] revealed a measurable hydrogen concentration, therefore suggesting an internal hydrogen embrittlement mechanism. The amount of H was not quantified because, as stated by the authors, the method also sensed H contained in surface corrosion products formed as a consequence of air exposure after removal from the H_2 autoclave. However, the amount of H in the surface film could have been quantified with, for example, a blank control test on a sample not pre-charged in H_2.

Pre-exposure to corroding solutions.—Hydrogen permeation experiments performed in steels at a potential of −0.45 V_{SHE} suggest that it is possible to achieve hydrogen surface concentrations more than two orders of magnitude higher during cathodic charging than during gaseous H_2 charging at 100 kPa.[96] The corrosion potential of magnesium can be about 1 V lower than that value.[22] Thus, a high hydrogen fugacity on the magnesium surface is expected during aqueous corrosion,[6] with hydrogen diffusing into the lattice.

Samples exposed to distilled water at OCP[12,97] or at a cathodic potential,[97] or exposed to sulfate solutions under an applied cathodic potential[1,98] did not exhibit ductility loss in a subsequent slow strain rate test (SSRT) in air. Pitting or localized corrosion[1,9,12,13,99] during pre-exposure is required to cause embrittlement. However, this raises a question about the role of pits on HE: do pits provide film-free areas for hydrogen absorption or do they act as stress raisers? This was later clarified in some solutions by comparing mechanical properties after pre-exposure and after pre-exposure followed by dry air[1] or vacuum annealing,[13] as will be discussed later. Chakrapani and Pugh[13] studied the embrittlement of a Mg-7.5 wt% Al alloy after exposure to a solution containing 4 wt% NaCl and 4 wt% K_2CrO_4. The elongation to fracture and UTS measured by SSRT in air decreased with the amount of pre-exposure time at E_{OC}, Figure 4, which was accompanied by a continuous increase in absorbed hydrogen concentration with exposure time. Samples charged with hydrogen exhibited strain-rate dependent elongation and UTS,[13] and the fracture surfaces were cleavage-like. Moreover, energy dispersive X-ray spectroscopy (EDS) analysis of crack surfaces after SSRT revealed the absence of chloride, suggesting that: i) the observed cleavage-like surfaces were, in fact, cracks developed during SSRT in air and ii) they did not occur due to an anodic dissolution process during pre-exposure.

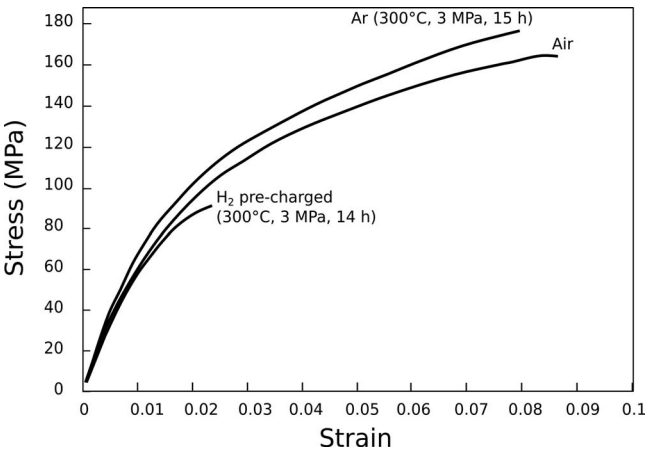

Figure 3. Slow strain rate tests performed in air on an AZ91 Mg-Al-Zn alloy heat treated in gaseous H_2 and Ar at 300°C and 3 MPa, compared to a control non-charged sample tested in air. (From reference 21, Mater. Sci. Eng., A, 488, Winzer, A. Atrens, W. Dietzel, V. S. Raja, G. Song, and K. U. Kainer, "Characterisation of stress corrosion cracking (SCC) of Mg–Al alloys" p. 339 (2008). Reproduced with permission of Elsevier S.A.).

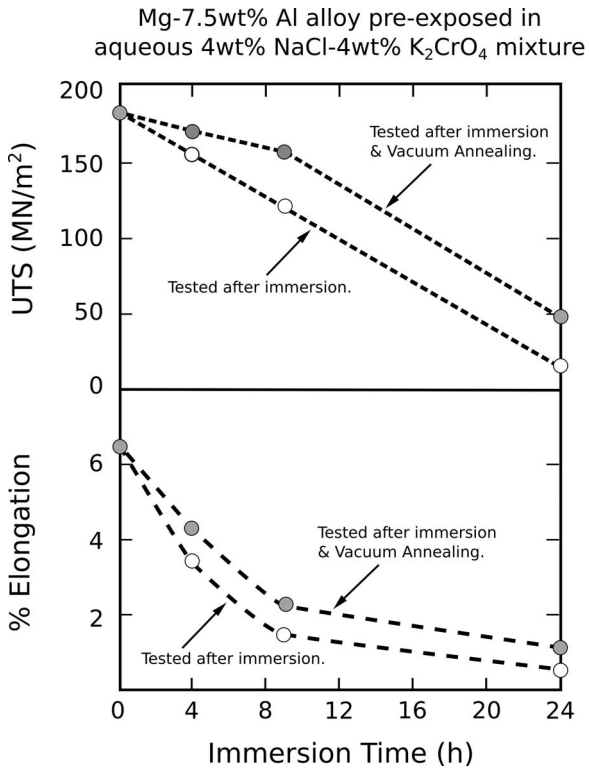

Figure 4. Evolution of ultimate tensile strength and elongation, measured in air, with pre-exposure time using SSRT, for a Mg-7.5 wt% Al alloy pre-exposed in aqueous 4 wt% NaCl-4 wt% K_2CrO_4 mixture, after Chakaprani and Pugh.[13] Results also show the increase in mechanical properties after a 4h vacuum annealing heat-treatment conducted at 385°C. (Reproduced from Metallurgical Transactions A, 7A, (1976), 173–178, "Hydrogen Embrittlement in a Mg-Al Alloy," D.G. Chakrapani and E.N. Pugh, Figure 2, with kind permission from Springer Science+Business Media B.V.).

Partial recovery in UTS and elongation to fracture was measured by Chakrapani and Pugh after vacuum annealing[13] pre-charged samples, Figure 4. As shown by the authors, the fracture surface was predominantly dimpled, and a reduction in H concentration was observed as determined by the inert gas fusion method.[13] Those results suggest a net contribution of hydrogen embrittlement to the SCC process. However, the dependence of UTS and ductility of the vacuum heat treated samples with exposure time also suggests an important irreversible effect during exposure to the environment, most likely related to a decrease in cross section or to localized corrosion causing stress concentration effects. In this regard, localized corrosion of Mg-Al alloys in chromate-chloride solutions proceeded with deep, tubular shaped pits.[100] Furthermore, the authors did not perform a control test to discard secondary effects such as grain growth or coarsening during the vacuum heat-treatment, both of which can have a direct effect on ductility and UTS.

Stampella[1] also reported complete reduction in ductility on unstressed pre-charged pure Mg samples during in air SSRT at OCP or at an anodic potential in a pH 10 sodium sulfate solution. However, in this case, given that mechanical properties were almost completely recovered after exposing pre-charged samples to dry laboratory air and allowing hydrogen to diffuse out, stress concentration effects or anodic dissolution contributions associated with the presence of localized corrosion were minimum. In these conditions, pits tended to grow larger in diameter than in depth,[1] minimizing stress concentration effects.

Environmental hydrogen embrittlement.—

Embrittlement in gaseous hydrogen.—Slow crack growth was observed in Mg-7.5 wt% Al alloy specimens tested in gaseous hydrogen,[13] resulting in a fracture surface similar to that obtained after hydrogen charging in a NaCl-K_2CrO_4 solution followed by in air testing. Similarly, a decrease in the reduction of area and UTS during SSRT of a Mg-8.8 wt% Al alloy in H_2 was reported.[69] The reduction in area after a tensile test, which is a direct indication of ductility, decreased with a decrease in strain rate.[69] The loss of ductility was higher when the sample was held in the environment prior loading, which allows longer times for hydrogen charging and transport.

SCC in aqueous solutions.—In order to lower uniform corrosion rates, SCC studies are generally conducted at high pH, distilled water, or in the presence of passivating ions such as chromates.[1–3,9,69] Pure magnesium has a general corrosion rate of approximately 0.2 μm/year in chromate solutions,[9] which is 30,000 times lower than the uniform corrosion rate in 100 ppm NaCl-containing solutions.[57] Chromate/chloride mixtures were extensively used in early investigations to simulate attack by chlorides to a chromate inhibited surface. However, it has been criticized that fully immersed short-term accelerated tests in chloride/chromate mixtures do not predict SCC reliably in practice.[101]

SCC of Mg-Al-Zn alloys was reported in conditions where localized corrosion was minimum, e.g. in distilled water at OCP[5,12,21,102,103] or at a net cathodic overpotential[97] and in chloride solutions at a net cathodic overpotential.[88] Those scenarios suggest SCC was possible even in situations where localized corrosion was negligible. Apparently,[97,103] in those cases, mechanical rupture of the surface film facilitated hydrogen absorption.

In the presence of corrosion inhibitors, such as potassium chromate (which participates in the formation of protective films[69]), Mg-Al alloys exhibited maximum SCC susceptibility at intermediate strain rates.[20,69] At very high strain rates, ductile failures were observed before the electrochemical reactions required for embrittlement could take place. In contrast, at very slow strain rates, the re-filming reaction at pits and bare metal zones was fast enough to prevent hydrogen absorption and crack propagation. The strain rate for maximum SCC susceptibility was, therefore, dependent on the chromate/chloride ratio.[69]

Effect of Second Phase Particles

Aluminum is perhaps the most common alloying element in magnesium alloys. Mg and Al form an eutectic system, with a maximum solubility of 12 mass-% of Al in Mg at the eutectic temperature, 436°C.[104] Al solubility is as low as 1 mass-% at room temperature.[104] β phase $Mg_{17}Al_{12}$ is a brittle intermetallic compound that precipitates in Mg-Al alloys above the solubility limit of Al in Mg. Jones et al.[11] studied SCC of a Mg-5 wt% Al alloy in 3.5% NaCl with 0.01 M K_2CrO_4. While some samples were solution heat treated and quenched, others had an additional artificial aging treatment at 200°C that resulted in precipitation of $Mg_{17}Al_{12}$, primarily at grain boundaries. Precipitation of this phase resulted in a shift from transgranular to intergranular crack modes as well as in an increase in crack growth rate by a factor of 1,800, despite a decrease in the applied stress intensity factor.[11] Such results contrast with those by other researchers who reported that intergranular cracking of Mg-Al alloys occurred at stresses higher than those observed in transgranular cracking.[18,20] Fairman and West[18] also suggested that aging promotes intergranular failure due to β phase precipitation, in accord with Wearmouth et al.,[20] as long as the grain size was small enough so that cracks could be oriented at an angle of 90° with respect to the tensile axis.

Jones et al. demonstrated, using polarization curves, that $Mg_{17}Al_{12}$ particles have an E_{OC} about 0.25 V higher than the E_{OC} of the matrix.[11] The authors suggested that during SCC the surrounding Mg matrix cathodically protects such particles. Crack advance between particles was suggested to be induced by H, but it could not be resolved whether crack propagation around particles occurred by anodic dissolution of the particle-matrix interface or by H-induced crack growth across the particle or at the particle matrix-interface.[11] The lack of passivation and generalized corrosion of the alloys in the solution used by Jones

made this issue difficult to discern,[11] preventing an analysis of the crack surface. Studying IGSCC of Mg-Al alloys in chromate solutions, Fairman and Bray[16] suggested that breakdown of the protective film could be facilitated by the presence of second phase particles. Studies on rare-earth containing magnesium alloys also concluded that precipitates promoted IGSCC by a galvanic effect.[4] It has been shown[22] that all key intermetallic particles present in common commercial magnesium alloys, with the exception of Mg_2Ca, are nobler than the magnesium matrix.

Winzer et al.[21] studied SCC of AZ91 (UNS M11910) alloy, which also contained β phase, in distilled water. Optical microscopy revealed cracks nucleated inside this phase oriented normally to the loading direction. Based exclusively on this evidence, Winzer et al. proposed a mechanism where SCC in AZ91 alloy proceeds by: i) hydrogen diffusion, followed by ii) hydrogen trapping by β particles ahead of the crack tip, iii) cracking, iv) release of hydrogen due to a decrease in stress, and v) hydrogen redistribution.[21] Studying the same alloy, Chen et al.[77] obtained SIMS images showing hydrogen enrichment in the eutectic region, and in β phase particles. The authors proposed that MgH_2 and hydrogen gas were responsible for cracks observed in this phase after cathodic charging in the absence of external loading. These conclusions were based solely on SIMS observations after cathodic charging followed by vacuum annealing at temperatures above and below a critical temperature, related to the MgH_2 decomposition temperature. Results were presented based on elemental distribution maps, from which phase information is difficult to extract. The authors assumed that any hydrogen removed above this temperature was due to MgH_2, while hydrogen not removed above this temperature corresponded to gaseous hydrogen. In carbon steels, where hydrogen effects have been studied in greater detail, it is known that hydrogen can be present in reversible and irreversible traps, each trap having a characteristic energy.[41] Hydrogen release occurs if the sample is annealed above a critical temperature. The presence of irreversible and reversible H traps in magnesium alloys could also explain the SIMS data shown by Chen et al.[77]

In a later study, scanning electron microscopy (SEM) examinations of H-charged AZ91 specimens[105] revealed hydrogen blisters surrounded by micro-cracks in adjacent β phase particles, which were presented as further evidence to support the presence of gaseous hydrogen. Circular spots on SEM images were identified as blisters, but a cross section analysis might have been better suited to identify such defects in more detail.

Hydrogen Embrittlement Mechanisms in Magnesium Alloys

A discontinuous crack propagation process has been reported for hydride forming metals such as Nb, V, Ta, Zr and Ti.[106,107] At temperatures where the hydride phase is stable, this phenomenon can be explained by the precipitation of hydrides ahead of the crack tip followed by fracture of this phase with arrest at the metal-matrix interface,[107] a mechanism known as delayed hydride cracking (DHC). Precipitation of hydrides, which have an increased volume per metal atom than the metal lattice, can be aided by the triaxial state of stress at the crack tip.[107]

When conditions for hydride precipitation are not met, or for non-hydride-forming materials, possible hydrogen-metal interactions proposed to cause embrittlement include adsorption-induced dislocation emission (AIDE), hydrogen-enhanced localized plasticity (HELP) and hydrogen-enhanced decohesion (HEDE). Details of these mechanisms are reviewed elsewhere.[107,108] There has been controversy regarding which of those processes dominates crack propagation, due in part to the fact that it is not possible to observe crack tips in the bulk of a material at atomic scale.[109] Therefore, mechanistic studies rely mainly on post-mortem analysis or on theoretical modeling.[110] In addition, fracture surfaces are often corroded, complicating the analysis even further,[109] especially for active metals like magnesium.

The lack of reliable hydrogen diffusion data in magnesium has prevented precise estimations of crack growth rates with the DHC mechanism.[23] Furthermore, crack growth rates expressions do not exist for all hydrogen induced cracking mechanisms,[110] which makes it difficult to discern between them. However, it could be stated that mechanisms that require hydrogen diffusion, such as HELP, HEDE or DHC, cannot operate at a rate faster than that required for hydrogen diffusion ahead of the crack tip, in contrast to AIDE, which only requires hydrogen adsorption.[108]

Evidence for each mechanism related to magnesium and its alloys is discussed below.

Delayed hydride cracking (DHC).— Precipitation and fracture of hydrides plays a major role in zirconium, titanium and its alloys,[67] which are hcp metals that form stable hydrides. Magnesium is also an hcp hydride-forming material, but MgH_2 is not as stable as hydrides of zirconium and titanium[67] and it decomposes at temperatures above 287°C,[25] under a H_2 pressure of 101.3 kPa.

Complications associated with detection of MgH_2 in fracture surfaces.—Hydrides are not always observed in the fracture surface[106] because stress is relieved after cleavage and the phase might become unstable in the absence of stress, causing hydrogen to return to solid solution. Further complications specific to MgH_2 include: i) decomposition under the electron beam in the transmission electron microscope (TEM)[31,111] and SEM[112] and ii) reaction of MgH_2 with water or ambient humidity yielding $Mg(OH)_2$ and H_2.[31,32]

Role of MgH_2 in stress corrosion cracking.—While there is evidence suggesting that MgH_2 might be present in the surface film formed during corrosion of magnesium and its alloys, as previously reviewed, its role during SCC is not clear. Several authors[3,5,9,13,23] have speculated about the role of brittle hydrides during SCC, but there is no conclusive evidence to support a hydride-based mechanism for Mg and Mg-alloys. Strong evidence[113] for the acceptance of this mechanism, such as the presence of hydrides on both halves of cleavage-like fractures with crack arrest markings near the hydrides-metal matrix interface, has not yet been found for magnesium or magnesium based alloys, despite several attempts.[9,15]

Winzer et al.[23] proposed a DHC mechanism involving hydrogen diffusion to the crack tip assisted by: i) concentration and stress gradients, ii) hydride precipitation when the H *solvus* is exceeded, and iii) fracture of the hydride when it exceeds a critical size. Modeling was complicated due to the fact that the diffusion coefficient and H *solvus* concentration in Mg as well as the critical hydride size were not known with enough precision.[23] Regardless of these limitations, the authors reported an estimated crack growth rate of 10^{-7} m/s, which was in the right order of magnitude for SCC in pure water but too low to explain SCC in other environments, such as those reported for Mg-Al alloys in chloride chromate mixtures.[14,20] This calculation assumed a "virgin" material, i.e. one in which the initial hydrogen concentration ahead of the crack is zero.[23] However, faster crack growth rates could be obtained if the crack propagated in a region with pre-charged hydrogen.[23]

A "quasi-porous" fracture surface, was observed in AZ91 magnesium alloy specimens pre-charged in H_2 at 300°C and 3 MPa for 16 h and then tested by SSRT at room temperature.[5] At this H_2 pressure, MgH_2 decomposes at around 427°C,[27] thus, the heat-treatment was performed in the region where hydrides were stable. However, no direct evidence supporting the presence of hydrides was found in SEM examinations of the fracture surfaces.[5]

Given the high H supersaturation due to the decrease in temperature, the absence of hydrides in fractographies was in contrast to thermodynamic predictions.[5,28] The authors[5] still proposed that the hydride-based hydrogen embrittlement mechanism[23] discussed previously was applicable, but with an additional step to account for the re-dissolution of hydrides after their fracture, resulting in the formation of the observed porous surface.

The supersaturation at room temperature after pre-charging at 300°C as well as the decrease in elastic energy due to the elastic stress field present during SSRT testing are the main driving forces for MgH_2 precipitation. However, the authors recognized that the effect of stress was small compared to the effect of cooling.[5] Therefore,

it is not clear what triggers the "re-dissolution" of MgH_2 after fracture to yield a void on the surface. Tests were performed in air where formation of such pores could not be promoted by electrochemical dissolution of MgH_2. The formation of such pores by solid-state diffusion would require room temperature diffusion of hydrogen and magnesium and would increase the surface area of the metal-air interface, an unlikely process contrary to thermodynamic predictions. Other possibilities not acknowledged by the authors are degradation of the hydrides due to exposure to environmental humidity[31] during manipulation of the fractured samples or decomposition of the phase under the SEM electron beam.[112]

Schober[31] presented direct evidence of MgH_2formation under charging in gaseous H_2 at 5 MPa, 270°C and 16 h. Those conditions are very similar to those used by Winzer et al.,[5] and also correspond to a region where MgH_2 is stable.[27] However, Schober charged TEM thin films after the final electropolishing step was finished, minimizing the damage to MgH_2. TEM bright field micrographs combined with selective area diffraction patterns (SAD), performed with a nitrogen cooled stage, confirmed the presence of blocky MgH_2 particles, of about 1 to 50 μm in size.[31] Cracks were observed in the periphery of hydrides once they exceeded a critical size of ∼5–10 μm. After deliberate in-situ heating to 250°C, hydrides decomposed and caused the deterioration of the microscope vacuum, probably due to the released H_2. Those results suggest that stresses were not required for hydride precipitation under those conditions. Given the similar charging conditions adopted by Winzer et al. and Schober, stresses were probably not required for the AZ91 samples used by Winzer et al.[5] This further suggests that re-dissolution of hydrides after their fracture is unlikely under those charging conditions.

Perhaps the most direct evidence of deterioration of mechanical properties by hydride formation is that presented by El-Amoush,[10] who charged 0.5 mm thick Mg-Al samples in hydrogen plasma for 30 min at 120°C. After this process, the author identified by XRD a layer containing MgH_2 in Mg-5 wt% Al samples and MgH_2 and AlH_3 in Mg-15 wt% and Mg-30 wt% samples. YS, UTS and ductility decreased for the hydrogen charged samples. A decrease in these properties of approximately 5% was found for the Mg-5 wt% Al alloy. This percentage increased with the Al content of the alloy.[10] Hydride formation caused increased surface hardness, and the depth of the surface hardened layer increased with Al content. This is in accord with the improvement of hydrogen absorption kinetics by Al, which enhances Mg solid state hydrogen storage capabilities.[24,33] However, despite the undisputed presence of hydrides in the Mg-5 wt% Al sample, the reported decrease in mechanical properties is low if compared to the values suggested by other investigators, Figure 3. This could be related to the relatively thin hydrided layer in this sample (i.e. approximately 100 μm[10]).

Adsorption-induced dislocation emission (AIDE).— The AIDE mechanism is based on a decrease of the interatomic bond energy induced by H at the crack tip, which facilitates the subsequent emission of dislocations.[108] The mechanism involves shear movement of atoms facilitated by H adsorption leading to the simultaneous formation of a slip step at the crack tip and a dislocation core,[110] Figure 5. The process occurs at high stresses ahead of the crack tip, which results in voids at slip band intersections or particles.

Slip from crack tips combined with coalescence of voids ahead of cracks result in crack growth. This model predicts fracture surfaces parallel to crystallographic planes that bisect the angle between the slip planes. Fractures surfaces should be covered by dimples or flutes, which are tubular voids nucleated at the intersection of slip bands, Figure 6. Those features can be so small that are sometimes resolved only in the atomic force microscope (AFM) or replicas observed in the transmission electron microscope.[108] Void formation ahead of the crack is essential for maintaining a sharp crack tip, because crack propagation exclusively by slip would result in a constant crack-tip angle,[114] which is not observed in practice.

Lynch and Trevena[2] conducted tensile tests on pure magnesium in dry air, chloride/chromate mixtures, and liquid alkali metals. Air frac-

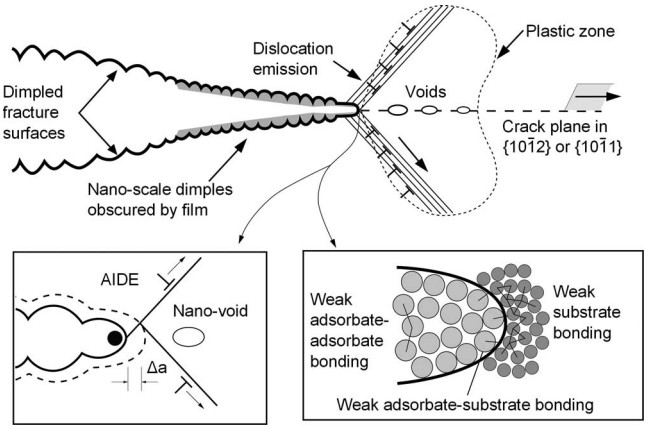

Figure 5. Schematics of processes leading to hydrogen assisted cracking by the adsorption-induced dislocation emission mechanism (AIDE), adapted from[110] with permission of Woodhead Publishing Limited.

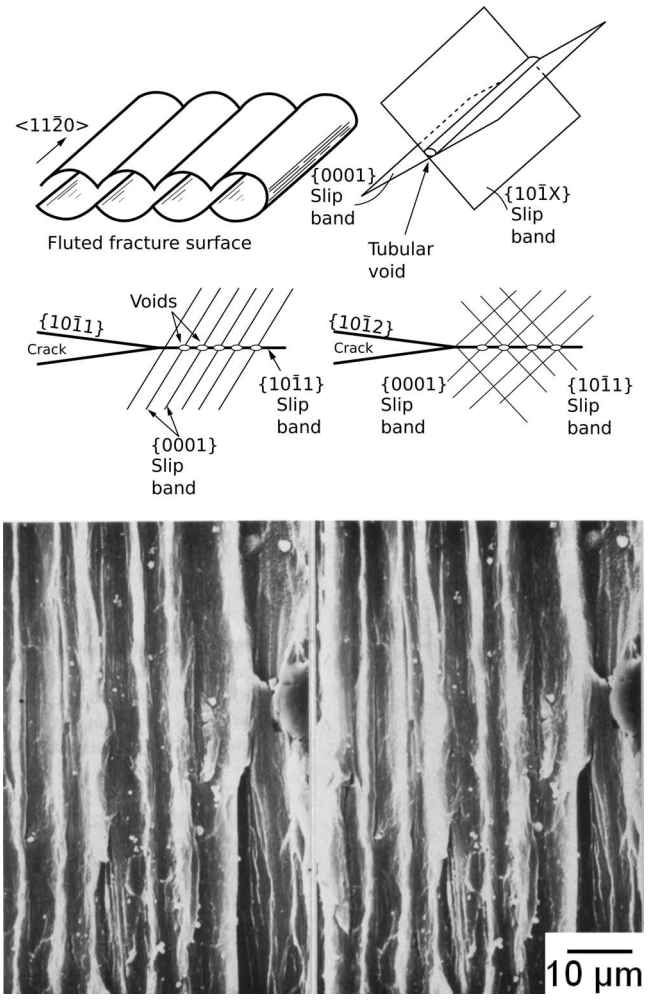

Figure 6. Diagram illustrating the formation of fluted $(10\bar{1}X)$ fracture surfaces and flutes observed by SEM in fracture surfaces after SCC of pure magnesium in chloride-chromate mixtures. From reference 2, S. P. Lynch and P. Trevena, "Stress corrosion cracking and liquid metal embrittlement in pure magnesium," Corrosion, 44, 113–124 (1988), ©NACE International 1988.

ture by overload resulted in "fluted" transcrystalline facets parallel to $(10\bar{1}X)$ pyramidal planes, with X near 1, and dimpled intercrystalline facets.

Fracture in liquid alkali metals and aqueous environments resulted in smaller and shallower flutes and dimples, indicating a more localized process, Figure 6. Liquid alkali metals[2] had negligible solubility in magnesium at the testing temperature and did not form intermetallic compounds, therefore, adsorption was the only interaction possible in this case.

Fractographies of liquid metal embrittlement (LME) were similar to those obtained after SCC, suggesting that hydrogen adsorption and liquid metal adsorption could be the rate controlling step in the fracture process. The authors proposed that adsorption of hydrogen or alkali metals facilitate the emission of dislocations from the crack tip, which promoted the coalescence of cracks with voids.[2] Microdimples on cleavage-like facets were also observed by Winzer et al.[5] in an AZ31 alloy tested in distilled water, but since the plane of the facet was not identified, it is difficult to conclude if the mechanism was HELP or AIDE.

Fracture surfaces presented by Lynch and Trevena[2] for SCC of pure magnesium in chloride-chromate mixtures when the crack velocity was 10^{-6} cm/s were similar to those obtained when it was on the order of 5 cm/s. Those different crack velocities were obtained by changing the strain rate of the test. The same mechanism was deduced to be operating at both rates, due to similarities in fracture surfaces. HEDE, HELP, and DHC require a hydrogen atmosphere ahead of the moving crack, which cannot be sustained if the ratio of hydrogen diffusion coefficient to crack velocity, D_H^{Mg}/v, is lower than 10^{-8} cm.[8,86] Therefore, assuming $D_H^{Mg} = 10^{-9}$ cm^2/s as obtained by Renner and Grabke,[43] HEDE, HELP, and DHC were discarded because only adsorption of hydrogen was possible at the higher crack growth rate.[2] However, Atrens[44] recently questioned that using $D_H^{Mg} = 10^{-5}$ cm^2/s, obtained after extrapolating Nishimura[42] results to room temperature, hydrogen diffusion could be possible ahead of the crack tip. Furthermore, the D_H^{Mg}/v criteria does not take into account hydrogen transport assisted by dislocations, which can be faster than lattice diffusion.[115]

Other authors[3] also observed cracks growing along $(10\bar{1}X)$ planes in pure magnesium with fluting in some cases, but suggested a cleavage-based mechanism to explain crack growth. According to the authors, crack growth was assisted either by high hydrogen concentrations that reduce surface energy of crystallographic planes or by nucleation of hydrides, but those phases were not detected. Reduction of surface energy in the presence of hydrogen is a thermodynamic statement that does not provide a mechanism, as suggested by Oriani.[114] Chakaprani and Pugh[14] observed fractures parallel to the $(10\bar{1}X)$ plane during liquid nitrogen cleavage, but during SCC of pure magnesium in chloride/chromate mixtures, cracks were parallel to $(31\bar{4}0)$. The authors speculated[13] that this could be the cleavage plane of a hydride. An argument for the cleavage mechanism[3] was that opposing fracture surfaces were interlocking, a feature that was also observed by other authors.[14] An opposing matching and interlocking fracture surface cannot be produced by a mechanism that predicts dimples and flutes due to dislocation activity, Figure 6. However, Lynch[2] mentioned that sometimes those features are only resolved at high resolution, whereas at lower resolution (as determined by SEM) surfaces can appear featureless. Continuous crack growth was observed by Lynch,[2] in contrast to Chakaprani and Pugh results, where crack arrest markings, Figure 7, and discrete peaks during acoustic emission suggested discontinuous crack growth.[14]

Hydrogen-enhanced decohesion (HEDE).— This model is based on hydrogen decreasing the metal-metal bond energy at the crack tip region.[108] Fracture proceeds when the local stress exceeds the cohesive strength of the H weakened bonds.[107] Hydrogen in solid solution is present as an interstitial in octahedral sites in the magnesium lattice.[37] Therefore, there is a driving force for its transport to the crack tip zone, where the high hydrostatic stresses would decrease the strain

Figure 7. TEM replica of a Mg-7.6 wt% Al alloy SCC fracture surface tested in chloride-chromate mixtures showing fine parallel markings (A), which represent the successive position of the crack tip during discontinuous crack propagation, after Chakrapani and Pugh.[14] (Reproduced from Metallurgical Transactions A, 6A, (1975), 1155-1163, "The Transgranular SCC of a Mg-Al Alloy: Crystallographic, Fractographic and Acoustic-Emission Studies," D.G. Chakrapani and E.N. Pugh, Figure 9, with kind permission from Springer Science+Business Media B.V.).

energy associated with its dissolution. Fracture can proceed along cleavage planes in matrix or particles, particle-matrix interfaces or grain boundaries. This model predicts featureless crack surfaces with no evidence of local plasticity,[107] except for steps or tearing between de-cohered regions.[108] A major limitation of this model is that there are difficulties in measuring the cohesive force and modeling is the only viable option.[107]

Hydrogen segregation at triple junctions of grain boundaries was detected by SIMS on pure magnesium samples with hydrogen in the 16-35 ppm range.[87] At those concentrations, which are about 1 order of magnitude lower than those reported by pre-charging in chromate-chloride mixtures,[13] hydrogen did not affect tensile properties, as reported for the samples pre-charged in chromate-chloride mixtures,[13] but caused an increase in the ductile to brittle transition temperature and increased tendency to intergranular fracture. First principles simulations of H segregation to Mg grain boundaries also concluded that at low concentrations tensile properties are not affected.[116]

Stampella et al.[1] adopted the HEDE model to explain the embrittlement observed in commercially and highly pure magnesium. When embrittlement was observed during SSRT experiments, fractographies revealed transgranular quasi-cleavage fractures, which were mixed, in some cases, with brittle intergranular cracks. The authors showed that fractographies obtained during SCC were similar to those obtained after brittle fracture in liquid nitrogen, and also reported no evidence of ductility or hydrides. Therefore, HEDE appeared to be the most viable mechanism.[1] It has to be noted that fractographic evidence was collected using SEM, even though some of the features that are usually evidence of dislocation motion, like shallow dimples, can only be resolved in the TEM or AFM.[108] Finally, the authors used the term "quasi-cleavage" to describe the fracture surface. The term "quasi-cleavage" *per se* is used to describe a failure along a non-cleavage plane, with river markings parallel to the crack propagation direction.[117] Therefore, those surfaces are indicative of localized dislocation activity, enhanced by hydrogen.[106,117]

Stampella et al.[1] observed that hydrogen embrittlement decreases after exposing pre-charged samples to a dry environment at room temperature. Therefore, the author pointed out that the mechanism should

not involve hydrides, because they have a much higher decomposition temperature (i.e. approximately 280°C). However, this decomposition temperature is valid under a hydrogen pressure of 101.3 kPa, and it is accepted that stresses at the crack tip can stabilize hydride formation, even when it is unstable in the absence of stress.[41]

Winzer et al.,[5,21] based on fractographic evidence, concluded that fracture of β particles in Mg-Al alloys proceeded by HEDE. Fracture of these particles was involved in the initiation and propagation of stress corrosion cracks. Alloy AZ91, which contains appreciable amount of β phase, was more susceptibility to SCC in distilled water than alloy AZ31 alloy, which has a similar matrix but a lower amount of precipitates.[21] However, it has to be stated that the authors compared AZ91 castings against AZ31 extrusions. HELP or AIDE were suggested for AZ31[5] alloy and AZ91[5,103] matrix, based on observation of microdimples and flutes.

Song et al.[99] also tested alloy AZ31 in different environments including distilled water and NaCl solutions. The fracture surface was quasi-cleavage mixed with intergranular cracking.[99] However, Winzer et al.[5] detected, in an independent work, microdimples on the fracture surface of AZ31, suggesting a dislocation based mechanism. The continuous decrease in mechanical properties with pre-exposure time, reported by Song et al.,[99] combined with the microdimples observed in the same alloy by Winzer et al.[5] would suggest contributions from HELP, which is based on dislocation motion and absorbed hydrogen. It is not clear why microdimples were observed by Winzer et al. but not by Song et al. Possible reasons could be a better resolution and smearing of features by corrosion. However this was not analyzed in depth by the authors.

Hydrogen-enhanced localized plasticity (HELP).— This model is based on dissolved hydrogen ahead of the crack tip decreasing the dislocation motion resistance and the flow stress, resulting in increased mobility of dislocations.[106,109] After admission of hydrogen in a specially designed cell, faster dislocation motion and a higher rate of dislocation creation from sources was observed in thin foils in-situ in the TEM.[106] A higher dislocation activity was observed for screw, edge, and mixed dislocations in fcc, hcp, and bcc crystals.[106,108] Due to the localization of stresses and hydrogen at the crack tip, plastic deformation becomes localized in this region, but the exact mechanism linking localized shearing with fracture is unknown.[106,108] Given that the process is extremely localized, the degree of plastic deformation remains very small macroscopically.[107] Reasons for the increased mobility of dislocations with hydrogen are based on hydrogen atmospheres around moving dislocations and obstacles, that can be reconfigured to minimize the energy of the system.[108] Interestingly, the model can predict dimpled fracture surfaces.[108]

Kuramoto et al.[118] suggested dislocation motion at the crack tip and detected hydrogen in slip bands using the hydrogen microprint technique,[119] in an AZ31 alloy stressed in a NaCl solution. Those observations are in accord with the HELP mechanism. Winzer et al.[5] also speculated about this mechanism controlling crack growth after observing microdimples in fracture surfaces of AZ31 and AZ91 magnesium alloys stressed in distilled water. In another study,[102] also performed on AZ31, Winzer et al. showed a decrease in the slope of the applied load vs. crack tip opening displacement curve from air to distilled water, which suggested an increased size of the plastic zone compatible with HELP. However, the microdimples observed in the same material tested in the same environment[5] were not observed this time.[102]

Concluding Remarks

Unless a significant contribution from hydrogen embrittlement is accepted, several aspects of Mg SCC cannot be fully understood. It is difficult to explain, for instance: i) the decrease in tensile properties observed in pure gaseous hydrogen, ii) the continuous decrease in mechanical properties with charging time, and iii) the partial recovery of mechanical properties after vacuum or dry-air storage of pre-charged specimens without considering a strong influence of hydrogen in crack propagation kinetics. In this regard, most authors agree that hydrogen embrittlement does play a role in the poor SCC resistance of magnesium and its alloys in various environments. However, there is still controversy on the fundamentals of the H-metal interactions responsible for the observed deterioration in mechanical properties.

Mg is a well-known hydride-forming element with applications to solid-state hydrogen storage. In hydrogen storage research, charging of magnesium to yield MgH_2 is usually performed at high temperature and pressure, usually on the order of 300–400°C and > 1 MPa. Mechanical testing of tensile specimens charged under such conditions exhibited hydrogen embrittlement.[102] Furthermore, MgH_2 was detected in the surface film of samples corroded in various environments, probably aided by the high concentration of hydrogen near the surface. MgH_2 reacts with water, suggesting that the phase could be created faster than it could be consumed due to corrosion. However, SEM and TEM examinations of *post-mortem* tensile specimens could not directly prove the presence of this phase near or at the fracture path. This is probably the strongest evidence against the acceptance of a delayed hydride cracking mechanism at room temperature. MgH_2 reacts with humidity and decomposes under the electron beam unless special precautions are taken, such as the use of a nitrogen-cooled stage and minimum exposure to water or ambient humidity of the H-charged specimens. It would be interesting to investigate whether hydride detection in the region close to the fracture path is possible by following those precautions that are well known to the hydrogen storage community.

Future research should also investigate the possible sites hydrogen can occupy in the magnesium lattice. At low concentration (16–35 ppm), hydrogen was mainly segregated to grain boundaries[87] and had a negligible effect on tensile properties.[87,116] Extrapolations to room temperature suggest that those values exceed the solubility of H in Mg. Therefore, it is not completely understood why hydrides were not detected in those samples. On the other hand, H charging by H plasma[10] resulted in a MgH_2 layer, clearly detected by XRD, that increased hardness and decreased the tensile properties of Mg-Al samples. However, the decrease in mechanical properties associated with this layer was rather mild if compared with the decrease obtained by other researchers [1,3,13,21] after exposure of magnesium and magnesium alloys to aqueous solutions. H charging due to corrosion in chloride-chromate mixtures resulted in intermediate hydrogen concentrations in the range of 100–200 ppm,[13] and up to 100 ppm due to exposure to water vapor exposure.[79] Thermodynamic predictions suggest that hydrogen should be precipitated in MgH_2 as a separate phase at those concentrations. Hydrogen could also reside inside the magnesium lattice as gaseous hydrogen in blisters or bubbles.[77,105] Thermal spectroscopy desorption studies, where the flow of hydrogen exiting the sample is measured during heating, could be useful for determining the possible states of hydrogen at concentrations relevant for corrosion.

Finally, a reliable value of the hydrogen diffusion coefficient in magnesium measured at room temperature is still required. This value is the key to quantify crack growth velocities due to any hydrogen embrittlement mechanism, with the exception of AIDE, which is based on hydrogen adsorption.

References

1. R. S. Stampella, R. P. M. Procter, and V. Ashworth, *Corros. Sci.*, **24**, 325 (1984).
2. S. P. Lynch and P. Trevena, *Corrosion*, **44**, 113 (1988).
3. E. Meletis and R. Hochman, *Corrosion*, **40**, 39 (1984).
4. M. Bobby Kannan, W. Dietzel, C. Blawert, A. Atrens, and P. Lyon, *Mater. Sci. Eng., A*, **480**, 529 (2008).
5. N. Winzer, A. Atrens, W. Dietzel, G. Song, and K. U. Kainer, *Metall. Mater. Trans. A*, **39**, 1157 (2008).
6. N. Winzer, A. Atrens, G. Song, E. Ghali, W. Dietzel, K. U. Kainer, N. Hort, and C. Blawert, *Adv. Eng. Mater.*, **7**, 659 (2005).
7. E. Ghali, *Uhlig's Corrosion Handbook* R. Winston Revie, Editor, John Wiley & Sons, (2000), p. 793–830.
8. S. P. Lynch, *Scr. Metall.*, **21**, 157 (1987).
9. G. L. Makar, J. Kruger, and K. Sieradzki, *Corros. Sci.*, **34**, 1311 (1993).
10. A. S. El-Amoush, *J. Alloys Compd.*, **463**, 475 (2008).

11. R. H. Jones, J. S. Vetrano, and C. F. Windisch, *Corrosion*, **60**, 1144 (2004).
12. M. Bobby Kannan and W. Dietzel, *Mater. Design*, **42**, 321 (2012).
13. D. G. Chakrapani and E. N. Pugh, *Metall. Trans. A*, **7**, 173 (1976).
14. D. G. Chakrapani and E. N. Pugh, *Metall. Trans. A*, **6**, 1155 (1975).
15. A. J. Bursle and E. N. Pugh, in *Mechanisms of environment sensitive cracking of materials. Proceedings of an international conference organized by the Metals Society*, p. 471–481, London (1977).
16. L. Fairman and H. J. Bray, *Br. Corros. J.*, **6**, 170 (1971).
17. L. Fairman and H. J. Bray, *Corros. Sci.*, **11**, 533 (1971).
18. L. Fairman and J. M. West, *Corros. Sci.*, **5**, 711 (1965).
19. R. Frankenthal, *Corros. Sci.*, **7**, 61 (1967).
20. W. R. Wearmouth, G. P. Dean, and R. N. Parkins, *Corrosion*, **29**, 251 (1973).
21. N. Winzer, A. Atrens, W. Dietzel, V. S. Raja, G. Song, and K. U. Kainer, *Mater. Sci. Eng., A*, **488**, 339 (2008).
22. A. D. Südholz, N. T. Kirkland, R. G. Buchheit, and N. Birbilis, *Electrochem. Solid-State Lett.*, **14**, C5 (2011).
23. N. Winzer, A. Atrens, W. Dietzel, G. Song, and K. U. Kainer, *Mater. Sci. Eng., A*, **466**, 18 (2007).
24. B. Sakintuna, F. Lamaridarkrim, and M. Hirscher, *Int. J. Hydrogen Energy*, **32**, 1121 (2007).
25. H. Okamoto, *J. Phase Equilib.*, **22**, 598 (2001).
26. A. San-Martin and F. D. Manchester, *Bull. Alloy Phase Diagrams*, **8**, 1987 (1987).
27. J. F. Stampfer, C. E. Holley, and J. F. Suttle, *J. Am. Chem. Soc.*, **82**, 3504 (1960).
28. F. D. Manchester and A. San-Martin, in *Phase Diagrams of Binary Hydrogen Alloys*, F. D. Manchester, Editor, p. 83–94, ASM International, Materials Park, OH (2000).
29. Z. Luz, *Scr. Metall.*, **14**, 275 (1980).
30. D. L. Douglass, *Metall. Mater. Trans. A*, **6**, 2179 (1975).
31. T. Schober, *Metall. Trans. A*, **12**, 951 (1981).
32. T. Schober and M. K. Chason, *Scr. Metall.*, **15**, 791 (1981).
33. S. Bouaricha, J. P. Dodelet, D. Guay, J. Huot, S. Boily, and R. Schulz, *J. Alloys Compd.*, **297**, 282 (2000).
34. A. Andreasen, *Int. J. Hydrogen Energy*, **33**, 7489 (2008).
35. P. Spatz, H. A. Aebiseher, A. Krozer, and L. Schlapback, *Z. Phys. Chem.*, **181**, 393 (1993).
36. A. Krozer and B. Kasemo, *Z. Phys. Chem.*, **164**, 1257 (1989).
37. K. Zeng, T. Klassen, W. Oelerich, and R. Bormann, *Int. J. Hydrogen Energy*, **24**, 989 (1999).
38. D. Talbot, *Int. Metall. Rev.*, **20**, 166 (1975).
39. Z. D. Popovic and G. R. Piercy, *Metall. Trans. A*, **6**, 1915 (1975).
40. A. Krozer and B. Kasemo, *J. Phys.: Condens. Matter*, **1**, 1533 (1989).
41. J. P. Hirth, *Metall. Trans. A*, **11**, 861 (1980).
42. C. Nishimura, M. Komaki, and M. Amano, *J. Alloys Compd.*, **293-295**, 329 (1999).
43. J. Renner and H. J. Grabke, *Z. Metallkunde*, **69**, 639 (1978).
44. A. Atrens, N. Winzer, G. Song, W. Dietzel, and C. Blawert, *Adv. Eng. Mater.*, **8**, 749 (2006).
45. T. Zakroczymski, *J. Electrochem. Soc.*, **132**, 2548 (1985).
46. S. Szklarska-Smialowska and Z. Xia, *Corros. Sci.*, **39**, 2171 (1997).
47. T. Zakroczymski, *Corrosion*, **41**, 485 (1985).
48. H. G. Schimmel, G. J. Kearley, J. Huot, and F. M. Mulder, *J. Alloys Compd.*, **404-406**, 235 (2005).
49. V. Knotek, V. Hošek, D. Vojtěch, P. Novák, J. Šerák, A. Michalcova, F. Průša, T. Popela, and M. Novák, in *Proceedings of the 19th International Conference on Metallurgy and Materials*, p. 1–6, Rožnov pod Radhoštěm, Czech Republic (2010).
50. M. A. V. Devanathan and Z. Stachurski, *Proc. R. Soc. London, Ser. A*, **270**, 90 (1962).
51. M. Danielson, *Corros. Sci.*, **44**, 829 (2002).
52. W. Dietzel, M. Pfuff, and N. Winzer, *Eng. Fract. Mech.*, **77**, 257 (2010).
53. A. Atrens, W. Dietzel, P. Srinivasan, N. Winzer, and M. Bobby Kannan, *Stress corrosion cracking (SCC) in magnesium alloys, Chapter 9 in Stress corrosion cracking: Theory and practice* V. S. Raja and T. Shoji, Editors, Woodhead Publishing, Oxford, (2011), p. 341–380.
54. H. Alves, U. Koster, E. Aghion, and D. Eliezer, *Materials Technology: Advanced Performance Materials*, **16**, 110 (2001).
55. P. Schmutz, V. Guillaumin, R. S. Lillard, J. A. Lillard, and G. S. Frankel, *J. Electrochem. Soc.*, **150**, B99 (2003).
56. N. Hara, Y. Kobayashi, D. Kagaya, and N. Akao, *Corros. Sci.*, **49**, 166 (2007).
57. R. Tunold, H. Holtan, M. Berge, A. Lasson, and R. Steen-Hansen, *Corros. Sci.*, **17**, 353 (1977).
58. G. Song and A. Atrens, *Adv. Eng. Mater.*, **5**, 837 (2003).
59. A. Turnbull, *Corros. Sci.*, **34**, 921 (1993).
60. A. Turnbull, *Corrosion*, **66**, 1 (2010).
61. P. Bruzzoni and R. Caravaglia, *Corros. Sci.*, **33**, 1797 (1992).
62. G. Williams and H. N. Mcmurray, *J. Electrochem. Soc.*, **155**, 340 (2008).
63. G. Song and A. Atrens, *Adv. Eng. Mater.*, **9**, 177 (2007).
64. D. Eaves, G. Williams, and H. N. McMurray, *Electrochim. Acta*, **79**, 1 (2012).
65. K. G. Adamson and D. S. Tawil, *Corrosion, Volume I, Metal/Environment Reactions* L. L. Shreir, R. A. Jarman, and G. T. Burstein, Editors, Butterworth-Heinemann, Wobum, MA, (1994), p. 4:98–4:115.
66. G. S. Frankel, *J. Electrochem. Soc.*, **145**, 2186 (1998).
67. D. Hardie, in *Environment-Induced Cracking of Metals*, R. P. Gangloff and M. B. Ives, Editors, p. 347–361, NACE International, Kohler, Wisconsin (1990).
68. J. C. Scully, *Corrosion, Volume I, Metal/Environment Reactions* L. Shreir, R. Jarman, and G. Burstein, Editors, Butterworth-Heinemann, Wobum, MA, (1994), p. 8:115–8:142.
69. K. Ebtehaj, D. Hardie, and R. N. Parkins, *Corros. Sci.*, **28**, 811 (1988).
70. G. G. Perrault, *J. Electroanal. Chem. Interfacial Electrochem.*, **51**, 107 (1974).
71. M. Pourbaix, *Atlas of Electrochemical Equilibria in Aqueous Solutions*, 2nd edition, NACE international, (1974).
72. G. G. Perrault, *J. Electroanal. Chem. Interfacial Electrochem.*, **27**, 47 (1970).
73. E. Gulbrandsen, *Electrochim. Acta*, **8**, 1403 (1992).
74. A. Seyeux, M. Liu, P. Schmutz, G. Song, A. Atrens, and P. Marcus, *Corros. Sci.*, **51**, 1883 (2009).
75. C. H. Brun, J. Pagetti, and J. Talbot, *Mémoires Scientifiques De La Revue De Métallurgie*, **73**, 659 (1976).
76. A. P. Nazarov, A. P. Lisovskii, and Y. N. Mikhailovskii, *Prot. Met.*, **25**, 606 (1989).
77. J. Chen, J. Wang, E. Han, J. Dong, and W. Ke, *Corros. Sci.*, **50**, 1292 (2008).
78. ASTM E 1447-09, Standard Test Method for Determination of Hydrogen in Titanium and Titanium Alloys by Inert Gas Fusion Thermal Conductivity /Infrared Detection Method, in *Annual Book of ASTM Standards*, Philadelphia, (2009).
79. G. I. Morozova, *Met. Sci. Heat Treat.*, **50**, 100 (2008).
80. M. W. Mallett, A. F. Gerds, and C. B. Griffith, *Anal. Chem.*, **25**, 116 (1953).
81. N. I. Zainal Abidin, A. D. Atrens, D. Martin, and A. Atrens, *Corros. Sci.*, **53**, 3542 (2011).
82. J. Chen, J. Dong, J. Wang, E. Han, and W. Ke, *Corros. Sci.*, **50**, 3610 (2008).
83. Z. Shi, J. X. Jia, and A. Atrens, *Corros. Sci.*, **60**, 296 (2012).
84. N. T. Kirkland, N. Birbilis, and M. P. Staiger, *Acta biomater.*, **8**, 925 (2012).
85. T. E. Crozier and S. Yamamoto, *J. Chem. Eng. Data*, **19**, 242 (1974).
86. H. H. Johnson, in *Hydrogen in Metals*, I. M. Bernstein and A. Thompson, Editors, p. 35–49, ASM (1974).
87. Y. Chino, D. Nishihara, T. Ueda, and M. Mabuchi, *Mater. Trans.*, **52**, 1123 (2011).
88. Y. Uematsu, T. Kakiuchi, and M. Nakajima, *Mater. Sci. Eng., A*, **531**, 171 (2012).
89. J. Galvele, in *Treatise on Materials Science and Technology*, J. C. Scully, Editor, p. 1–57, London (1983).
90. A. Sehgal, D. Lu, and G. S. Frankel, *J. Electrochem. Soc.*, **145**, 2834 (1998).
91. A. Atrens and W. Dietzel, *Adv. Eng. Mater.*, **9**, 292 (2007).
92. N. T. Kirkland, G. Williams, and N. Birbilis, *Corros. Sci.*, **65**, 5 (2012).
93. J. Światowska, P. Volovitch, and K. Ogle, *Corros. Sci.*, **52**, 2372 (2010).
94. G. S. Frankel, A. Samaniego, and N. Birbilis, *Corros. Sci.* (2013).
95. G. Pressouyre, *Acta Metall.*, **28**, 895 (1980).
96. M. Luppo and J. Ovejero-Garcia, *Corros. Sci.*, **32**, 1125 (1991).
97. M. Bobby Kannan, W. Dietzel, R. K. S. Raman, and P. Lyon, *Scr. Mater.*, **57**, 579 (2007).
98. J. Chen, J. Wang, E. Han, and W. Ke, *Mater. Sci. Eng., A*, **494**, 257 (2008).
99. R. G. Song, C. Blawert, W. Dietzel, and A. Atrens, *Mater. Sci. Eng., A*, **399**, 308 (2005).
100. H. Pickering and P. Swann, *Corrosion*, **19**, 373 (1963).
101. A. Froats, T. K. Aune, D. Hawke, W. Unsworth, and G. Hillis, *Corrosion of Magnesium and Magnesium Alloys, Metals Handbook*, 9th ed., Vol. 13, Corrosion J. R. Davis, Editor, ASM International, Materials Park, OH, (1987), p. 740–754.
102. N. Winzer, A. Atrens, and W. Dietzel, *Adv. Eng. Mater.*, **10**, 453 (2008).
103. N. Winzer, A. Atrens, W. Dietzel, G. Song, and K. U. Kainer, *Mater. Sci. Eng., A*, **472**, 97 (2008).
104. H. E. Friedrich, B. L. Mordike, and B. L. Eds., *Magnesium Technology Metallurgy, Design Data, Applications*, Springer, Germany, (2006).
105. J. Chen, M. Ai, J. Wang, E.-H. Han, and W. Ke, *Corros. Sci.*, **51**, 1197 (2009).
106. H. K. Birnbaum, in *Hydrogen Effects on Material Behavior*, N. R. Moody and A. W. Thompson, Editors, p. 639–658, TMS (1990).
107. A. Turnbull, *Corros. Sci.*, **34**, 921 (1993).
108. S. P. Lynch, in *Hydrogen Effects on Material Behavior and Corrosion Deformation Interactions*, N. R. Moody, A. W. Thompson, R. E. Ricker, G. W. Was, and R. H. Jones, Editors, p. 449–466, TMS (The minerals, metals & materials society) (2003).
109. S. P. Lynch, *Metall. Mater. Trans. A* **44**, 1209 (2012).
110. S. P. Lynch, *Mechanistic and fractographic aspects of stress-corrosion cracking (SCC), Chapter 1 in Stress corrosion cracking: Theory and practice*, V. S. Raja and T. Shoji, Editors, p. 3–89, Woodhead Publishing, Oxford (2011).
111. B. Paik, I. P. Jones, A. Walton, V. Mann, D. Book, and I. R. Harris, *Philos. Mag. Lett.*, **90**, 1 (2010).
112. S. D. Beattie, U. Setthanan, and G. S. McGrady, *Int. J. Hydrogen Energy*, **36**, 6014 (2011).
113. S. P. Lynch, *Hydrogen embrittlement (HE) phenomena and mechanisms, Chapter 2 in Stress corrosion cracking: Theory and practice*, V. S. Raja and T. Shoji, Editors, p. 90–130, Woodhead Publishing, Oxford (2011).
114. R. Oriani, *Corrosion*, **43**, 390 (1987).
115. J. C. Scully, in *Effect of hydrogen on behavior of materials, Proceedings of an international conference*, p. 129–149, Moran, Wyoming (1975).
116. M. Yuasa, D. Nishihara, M. Mabuchi, and Y. Chino, *J. Phys.: Condens. Matter*, **24**, 085701 (2012).
117. M. L. Martin, J. a. Fenske, G. S. Liu, P. Sofronis, and I. M. Robertson, *Acta Mater.*, **59**, 1601 (2011).
118. S. Kuramoto, I. Araki, and M. Kanno, *Keikinzoku/Journal of Japan Institute of Light Metals*, **51**, 397 (2001).
119. T. E. Perez and J. Ovejero Garcia, *Scr. Metall.*, **16**, 161 (1982).